Interlaminar Mode II Fracture Characterization

Marcelo F. S. F. de Moura

Departamento de Engenharia Mecânica e Gestão Industrial

Faculdade de Engenharia da Universidade do Porto

Rua Dr. Roberto Frias s/n, 4200-465 Porto, Portugal

Summary

Delamination is an important concern in the context of structural behaviour of laminated composite materials. It is known that delamination can diminish the stiffness and the strength of the material and promote structural failure. Delamination onset and growth is governed by interlaminar fracture toughness of the material. Delamination propagation is frequently dominated by mode II fracture; consequently interlaminar fracture characterization under mode II loading is fundamental to accurately predict the susceptibility of the material to delamination. However, there are several problems inherent to the usual tests employed for mode II interlaminar fracture characterization, e.g., unstable crack propagation and difficulties in crack monitoring during propagation. These issues are discussed in section 1.

In section 2 the most popular fracture characterization tests in mode II are presented. A brief description of each one is given, with emphasis on the advantages and drawbacks thereof. The application of the classical data reduction schemes to each test is also described in section 2.1. After a succinct bibliographic review it is concluded that the End Notched Flexure (ENF) and End Loaded Split (ELS) tests are the most suitable ones to fracture characterization of composites in mode II. However, the dependence of

measured G_{IIc} on the crack length measurements for those tests is emphasized. In order to overcome this serious disadvantage a new data reduction scheme based only on the specimen compliance is proposed in section 2.2. The method is applied with little differences to the ENF and ELS tests and provides a straightforward measurement of G_{IIc}. Moreover, the method also includes the Fracture Process Zone (FPZ) effect, which was verified to be non negligible under mode II loading. In section 2.3 the referred tests were numerically simulated using a cohesive mixed-mode damage model. Appropriate values of critical strain energy release rates in mode I, II and III respectively, were inputted in the model. The main objective was to verify the capacity of the proposed methodology on the replication of the introduced G_{IIc}. Excellent agreement was obtained for the two tests. The ENF test was proposed as the most suitable for the determination of G_{IIc} owing to its simplicity.

In section 3 the dynamic fracture characterization is discussed. The difficulties inherent in the conduct of experimental tests execution are highlighted. The determination of the dynamic fracture toughness of composites is useful when dynamic delamination propagation is the predominant failure mode. Several works of different authors are summarized. One of the remarkable points is related to the existence of a crack speed threshold value, below which the dynamic and quasi-static toughness values are similar. The majority of the authors indicate that fracture toughness tends to decrease with increasing crack speed.

The main conclusions of this contribution are summarized in section 4.

1. Introduction

The application of composite materials in the aircraft and automobile industries lead to the increase of research on the fracture behaviour of composites. One of the most significant mechanical properties of fibre reinforced polymer composites is its resistance to delamination onset and propagation. It is known that delamination can induce significant stiffness reduction leading to premature failures. Delamination can be viewed as a crack propagation phenomenon, thus justifying a typical application of fracture mechanics concepts. In this context, the interlaminar fracture characterization of composites acquires remarkable relevancy. There are several tests proposed in the literature in order to measure the interlaminar strain energies release rates in mode I, mode II and mixed mode I/II. Whilst the mode I has already been extensively studied and the Double Cantilever Test (DCB) test is universally accepted, the mode II is not so well studied, which can be explained by some difficulties inherent to experimental tests. Moreover, in many real situations delaminations propagate predominantly in mode II, as is the case of composite plates under low velocity impact (Choi et al., 1992). This gives relevancy to the determination of toughness propagation values instead of the initiation ones commonly considered in design. Some non negligible differences can be achieved considering the *R*-curve effects (de Morais et al., 2007). These issues make the fracture characterization in mode II an actual and fundamental research topic. However, problems related to unstable crack growth and to crack monitoring during propagation preclude a rigorous measurement of G_{IIc}. In fact, in the mode II fracture characterization tests the crack tends to close due to the applied load, which hinders a clear visualization of its tip. In addition, the classical data reduction schemes, based on beam theory analysis and compliance calibration, require crack monitoring during propagation. On the other hand, a quite extensive Fracture Process Zone (FPZ) ahead of crack tip exists

under mode II loading. This non negligible FPZ affects the measured toughness as a non negligible amount of energy is dissipated on it. Consequently, its influence should be taken into account, which does not occur when the real crack length is used in the selected data reduction scheme. To overcome these difficulties a new data reduction scheme based on crack equivalent concepts and depending only on the specimen compliance is presented in the next section. The main objective of the proposed methodology is to increase the accuracy of experimental mode II fracture tests on the G_{IIc} measurements. In fact, a rigorous monitoring of the crack length during propagation is one of the complexities of these tests.

2. Static mode II fracture characterization

There are three fundamental experimental tests used to measure G_{IIc}. The most popular one is the End Notched Flexure (ENF), which was developed for wood fracture characterization (Barrett et al., 1977). The test consists on a pre-cracked specimen under three point bending loading (see Fig. 2.1). Unstable crack propagation constitutes one of the disadvantages of the ENF test. Another possibility is the End Loaded Split (ELS) test which is based on cantilever beam geometry (see Fig. 2.1). Although the ELS test involves more complexities during experiments relatively to the ENF test, it provides a larger range of crack length where the crack propagates stably. In fact, the ENF test requires $a_0/L>0.7$ to obtain stable crack propagation (Carlsson et al, 1986), whereas in the ELS test $a_0/L>0.55$ is sufficient (Wang at al., 1996). However, both of these tests present a common difficulty related to the crack length measurement during the experimental test. Different methods have been proposed in literature to address these difficulties. Kageyama et al. (Kageyama et al., 1991) proposed a Stabilised End

Notched Flexure (SENF) test for experimental characterization of mode II crack growth. A special displacement gage was developed for direct measurement of the relative shear slip between crack surfaces of the ENF specimen. The test was performed under constant crack shear displacement rate, which guarantees stable crack propagation. Yoshihara et al. (Yoshihara et al., 2000) recommended the use of Crack Shear Displacement method (CSD) to obtain the mode II *R*-curve since the crack length is implicitly included in the CSD. Tanaka et al. (Tanaka et al., 1995) concluded that to extend the stabilized crack propagation range in the ENF test, the test should be done under a condition of controlled CSD. Although the CSD method provides the measurement of the mode II toughness without crack length monitoring, this method requires a servo valve-controlled testing machine and the testing procedure is more complicated than the one under the loading point displacement condition. Alternatively the Four Point End Notched Flexure test (4ENF) (Fig. 2.1) can be used to evaluate the mode II *R*-curve. This test does not require crack monitoring but involves a more sophisticated setup and larger friction effects were observed (Shuecker et al., 2000). In the following, a summary of the classical reduction schemes used for these experimental tests is presented.

2.1 Classical methods

2.1.1 Compliance Calibration Method (CCM)

The CCM is the most used. During the test the values of load, applied displacement and crack length (P-δ-a) are registered in order to calculate the critical strain energy release rate using the Irwin-Kies equation (Kanninen et al., 1985)

$$G_{\mathrm{IIc}} = \frac{P^2}{2B}\frac{dC}{da} \qquad [2.1]$$

where B is the specimen width and $C=\delta/P$ the compliance. In the ENF and ELS tests a cubic relationship between the compliance (C) and the measured crack length a is usually assumed (Davies et al., 2001)

$$C = D + m\,a^3 \qquad [2.2]$$

where D and m are constants. G_{IIc} is then obtained from

$$G_{\mathrm{IIc}} = \frac{3P^2 m\,a^2}{2B} \qquad [2.3]$$

For the 4ENF test a linear relationship (Yoshihara, 2004) between the compliance (C) and the measured crack length a is used

$$C = D + m\,a \qquad [2.4]$$

being D and m the respective coefficients. It should be noted that relations C=f(a) given by equations [2.2] and [2.4] are based on the beam theory approach, as it will be shown in the next sub-section. G_{IIc} is given by

$$G_{\mathrm{IIc}} = \frac{P^2}{2B}m \qquad [2.5]$$

The three tests require the calibration of the compliance in function of the crack length. This can be done by measurement of crack length during propagation or, alternatively, considering several specimens with different initial cracks lengths to establish the compliance–crack length relation, which is regressed by a cubic (equation [2.2]) and linear (equation [2.4]) functions.

2.1.2 Beam theory

Beam theory methods are also frequently used to obtain G_{IIc} in mode II tests. In the case of ENF test Wang and Williams (Wang et al., 1992) proposed the Corrected Beam Theory (CBT)

$$G_{IIc} = \frac{9(a + 0.42\Delta_I)^2 P^2}{16 B^2 h^3 E_1} \qquad [2.6]$$

where E_1 is the axial modulus and Δ_I a crack length correction to account for shear deformation

$$\Delta_I = h\sqrt{\frac{E_1}{11 G_{13}}\left[3 - 2\left(\frac{\Gamma}{1+\Gamma}\right)^2\right]} \qquad [2.7]$$

with

$$\Gamma = 1.18\frac{\sqrt{E_1 E_2}}{G_{13}} \qquad [2.8]$$

where E_2 and G_{13} are the transverse and shear moduli, respectively. In the ELS case a similar expression is proposed (Wang et al., 1992)

$$G_{IIc} = \frac{9(a + 0.49\Delta_I)^2 P^2}{4 B^2 h^3 E_1} \qquad [2.9]$$

For the 4ENF test the beam theory leads to the following equation (Silva, 2006)

$$C = \frac{d}{24 E_1 I}\left(18 d\, a - 20 d^2 + 60 L^2 - 6 d\, L\right) \qquad [2.10]$$

where I is the second moment of area and d represents the distance between each support and its nearest loading actuator (Fig. 2.1). Using equation [2.1] G_{IIc} can be obtained from

$$G_{IIc} = \frac{9}{16}\frac{P^2 d^2}{E_1 B^2 h^3} \qquad [2.11]$$

In summary, the application of beam theory to ENF and ELS tests involves the crack length, which does not occur in the 4ENF test. However, it should be emphasized that

4ENF setup is more complex. Also, friction effects (Shuecker et al., 2000) and system compliance (Davidson et al., 2005) can affect the results. Owing to these drawbacks of the 4ENF test, the ENF and ELS tests emerge as the most appropriate to fracture characterization of composites in mode II. In this context, a new data reduction scheme, not depending on the crack length measurements, is proposed in the following section for these experimental tests.

2.2 Compliance Based Beam Method (CBBM)

In order to overcome the difficulties associated to classical data reduction schemes a new method is proposed. The method is based on crack equivalent concept and depends only on the specimen compliance. The application of the method to ENF and ELS tests is described in the following.

2.2.1 ENF test

Following strength of materials analysis, the strain energy of the specimen due to bending and including shear effects is

$$U = \int_0^{2L} \frac{M_f^2}{2E_f I}\,dx + \int_0^{2L}\int_{-h}^{h} \frac{\tau^2}{2G_{13}} B\,dy\,dx \qquad [2.12]$$

where M_f is the bending moment and

$$\tau = \frac{3}{2}\frac{V_i}{A_i}\left(1 - \frac{y^2}{c_i^{\,2}}\right) \qquad [2.13]$$

where A_i, c_i and V_i represent, respectively, the cross-section area, half-thickness of the beam and the transverse load of the i segment ($0 \leq x \leq a$, $a \leq x \leq L$ or $L \leq x \leq 2L$). From the Castigliano theorem, the displacement at the loading point for a crack length a is

$$\delta = \frac{dU}{dP} = \frac{P\left(3a^3 + 2L^3\right)}{8E_f Bh^3} + \frac{3PL}{10G_{13}Bh} \qquad [2.14]$$

Since the flexural modulus of the specimen plays a fundamental role on the P-δ relationship, it can be calculated from equation [2.14] using the initial compliance C_0 and the initial crack length a_0

$$E_f = \frac{3a_0^3 + 2L^3}{8Bh^3}\left(C_0 - \frac{3L}{10G_{13}Bh}\right)^{-1} \qquad [2.15]$$

This procedure takes into account the variableness of the material properties between different specimens and several effects that are not included in beam theory, e.g., stress concentration near the crack tip and contact between the two arms. In fact, these phenomena affect the specimen behavior and consequently the P-δ curve, even in the elastic regime. Using this methodology their influence are accounted for through the calculated flexural modulus. On the other hand, it is known that, during propagation, there is a region ahead of crack tip (Fracture Process Zone), where materials undergo properties degradation by different ways, e.g., micro-cracking, fibre bridging and inelastic processes. These phenomena affect the material compliance and should be accounted for in the mode II tests. Consequently, during crack propagation a correction of the real crack length is considered in the equation of compliance [2.14] to include the FPZ effect

$$C = \frac{3(a + \Delta a_{\mathrm{FPZ}})^3 + 2L^3}{8E_f Bh^3} + \frac{3L}{10G_{13}Bh} \qquad [2.16]$$

and consequently,

$$a_{\mathrm{eq}} = a + \Delta a_{\mathrm{FPZ}} = \left[\frac{C_{\mathrm{corr}}}{C_{0\,\mathrm{corr}}}a_0^3 + \frac{2}{3}\left(\frac{C_{\mathrm{corr}}}{C_{0\,\mathrm{corr}}} - 1\right)L^3\right]^{1/3} \qquad [2.17]$$

where C_{corr} is given by

$$C_{corr} = C - \frac{3L}{10G_{13}Bh} \qquad [2.18]$$

G_{IIc} can now be obtained from

$$G_{IIc} = \frac{9P^2 a_{eq}^2}{16B^2 E_f h^3} \qquad [2.19]$$

This data reduction scheme presents several advantages. Using this methodology crack measurements are unnecessary. Experimentally, it is only necessary to register the values of applied load and displacement. Therefore, the method is designated as Compliance-Based Beam Method (CBBM). Using this procedure the FPZ effects, that are pronounced in mode II tests, are included on the toughness measurement. Moreover, the flexural modulus is calculated from the initial compliance and initial crack length, thus avoiding the influence of specimen variability on the results. The unique material property needed in this approach is G_{13}. However, its effect on the measured G_{IIc} was verified to be negligible (de Moura et al., 2006), which means that a typical value can be used rendering unnecessary to measure it.

2.2.2 ELS test

Following a procedure similar to the one described for the ENF test, the applied P-δ relationship is

$$\delta = \frac{dU}{dP} = \frac{P\left(3a^3 + L^3\right)}{2Bh^3 E_1} + \frac{3PL}{5BhG_{13}} \qquad [2.20]$$

In order to include the root rotation effects at clamping and the details of crack tip stresses or strains not included in the beam theory, an effective beam length (L_{ef}) can be achieved. In fact, considering in equation [2.20] the initial crack length (a_0) and the initial compliance (C_0) experimentally measured, it can be written

$$C_0 - \frac{3a_0^3}{2Bh^3E_1} = \frac{L_{ef}^3}{2Bh^3E_1} + \frac{3L_{ef}}{5BhG_{13}} \qquad [2.21]$$

To take account for the FPZ influence a correction to the real crack length (Δa_{FPZ}) should be considered. From equation [2.20] the compliance (C) during crack propagation can be expressed as

$$C - \frac{3(a+\Delta a_{FPZ})^3}{2Bh^3E_1} = \frac{L_{ef}^3}{2Bh^3E_1} + \frac{3L_{ef}}{5BhG_{13}} \qquad [2.22]$$

Combining equations [2.22] and [2.21], the equivalent crack length can be given by

$$a_{eq} = a + \Delta a_{FPZ} = \left[(C - C_0)\frac{2Bh^3E_1}{3} + a_0^3 \right]^{1/3} \qquad [2.23]$$

G_{IIc} can now be obtained from

$$G_{IIc} = \frac{9P^2a_{eq}^2}{4B^2h^3E_1} \qquad [2.24]$$

Following this procedure G_{IIc} can be obtained without crack measurement during propagation which can be considered an important advantage. Equation [2.24] only depends on applied load and displacement during crack growth. Additionally, the influence of root rotation at the clamping point and singularity effects at the crack tip are accounted for, through initial compliance C_0. During propagation, the effect of FPZ on the compliance is also included using this methodology. In this case (ELS test) it is necessary to measure the longitudinal modulus.

2.3 Numerical simulations

In order to verify the performance of the CBBM on the determination of G_{IIc} of unidirectional composites, numerical simulations of the ENF and ELS tests were performed. A cohesive mixed-mode damage model based on interface finite elements

was considered to simulate damage initiation and propagation. A constitutive relation between the vectors of stresses ($\boldsymbol{\sigma}$) and relative displacements ($\boldsymbol{\delta}$) is postulated (Fig. 2.2). The method requires local strengths ($\sigma_{u,i}$, i=I, II, III) and the critical strain energy release rates (G_{ic}) as inputted data parameters [8, 9]. Damage onset is predicted using a quadratic stress criterion

$$\left(\frac{\sigma_{\mathrm{I}}}{\sigma_{u,\mathrm{I}}}\right)^2+\left(\frac{\sigma_{\mathrm{II}}}{\sigma_{u,\mathrm{II}}}\right)^2+\left(\frac{\sigma_{\mathrm{III}}}{\sigma_{u,\mathrm{III}}}\right)^2=1 \quad \text{if} \quad \sigma_{\mathrm{I}}\geq 0$$
$$\left(\frac{\sigma_{\mathrm{II}}}{\sigma_{u,\mathrm{II}}}\right)^2+\left(\frac{\sigma_{\mathrm{III}}}{\sigma_{u,\mathrm{III}}}\right)^2=1 \quad \text{if} \quad \sigma_{\mathrm{I}}\leq 0 \qquad [2.25]$$

where σ_i, (i=I, II, III) represent the stresses in each mode. Crack propagation was simulated by a linear energy criterion

$$\frac{G_{\mathrm{I}}}{G_{\mathrm{Ic}}}+\frac{G_{\mathrm{II}}}{G_{\mathrm{IIc}}}+\frac{G_{\mathrm{III}}}{G_{\mathrm{IIIc}}}=1 \qquad [2.26]$$

Basically, it is assumed that the area under the minor triangle of Fig. 2.2 is the energy released in each mode, which is compared to the respective critical fracture energy represented by the bigger triangle. The subscripts *o* and *u* refer to the onset and ultimate relative displacement and the subscript *m* applies to the mixed-mode case. More details about this model are presented in de Moura et al. (de Moura et al., 2006).

Three-dimensional approaches (Fig. 2.3 and Fig. 2.4) were carried out to include all the effects that can influence the measured G_{IIc}. The interface elements were placed at the mid-plane of the specimens to simulate damage progression. Very refined meshes were considered in the region of interest corresponding to crack initiation and growth. The specimens' geometry and material properties and are listed in Tables 2.1, 2.2 and 2.3, respectively. An analysis of *G*'s distributions at the crack front showed a clear

predominance of mode II along the specimens' width, although some spurious mode III exists at the specimens edges (de Moura et al., 2006 and Silva et al., 2007). Appropriate values of critical strain energy release rates were considered for each of the three modes, respectively (see Table 2.3). Consequently, the efficacy of the proposed data reduction scheme can be evaluated by its capacity to reproduce the inputted G_{IIc} from the P-δ results obtained numerically.

The application of the CBBM is performed by three main steps. The first one is the measurement of the initial compliance C_0 from the initial slope of the P-δ curves (figure (2.5) or (2.7)). This parameter is then used to estimate the flexural modulus in the ENF test (equation [2.15]). The next step is the evaluation of the equivalent crack length (equations [2.17] or [2.23]) in function of the current (C) and initial compliance (C_0). Finally, the R-curves, figures (2.6) and (2.8), can be obtained from equations [2.19] and [2.24], respectively. It should be noted that crack propagation occurs after peak load in both tests. During crack growth P decreases with the increase of equivalent crack length. This originates a plateau on the R-curves, which corresponds to the critical strain energy release rate in mode II (G_{IIc}). These plateau values are compared with the reference value (figures (2.6) and (2.8)), which represents the inputted G_{IIc}. The excellent agreement obtained in both cases demonstrates the effectiveness of the CBBM as a suitable data reduction scheme to determine G_{IIc}, without crack length monitoring during propagation. As the ENF test is much simpler to execute than the ELS one, it can be concluded that using the CBBM, the ENF test is the most suitable for the determination of G_{IIc} and it should be considered as the principal candidate for standardization.

3. Dynamic mode II fracture characterization

The research on dynamic crack propagation in composites has become the focus of several authors in the recent years. The dynamic fracture characterization of composites is not easy to perform. In fact, it is experimentally difficult to induce high speed delamination growth in a simple and controlled manner (Guo et al., 1998). However, the determination of dynamic fracture toughness of composites is of fundamental importance in the prediction of the dynamic delamination propagation in composite structures. In addition, it is known that the impact delamination is mainly governed by mode II fracture (Wang et al., 1991). However, there are several unclear phenomena related to dynamic crack propagation. One of the most important issues is related to the influence of rate effects on the propagation of dynamic cracks. An example of this occurrence is the dynamic delamination propagation occurring in composites submitted to low velocity impact. In this case, rate effects in the FPZ can interact with the well known rate-dependency of polymers leading to a very complicated phenomenon. In addition, Kumar et al. (Kumar et al., 1993) verified that when glass fiber reinforced epoxy laminates are impacted, the total delamination area between the various plies multiplied by the quasi-static energy release rate exceeds the energy of the impacting mass. This suggests that under high crack speeds, delamination propagates at lower toughness which leads to larger damaged areas. In order to explain this behaviour, Maikuma et al. (Maikuma et al., 1990) suggest that the calculation of critical strain energy release rate should account for the kinetic energy (E_{kin}) in equation [2.1]

$$G_{IIc} = \frac{P^2}{2B}\frac{dC}{da} - \frac{dE_{kin}}{B\,da} \qquad [3.1]$$

The kinetic energy expression can be obtained from

$$E_{\text{kin}} = \frac{1}{2}\rho B\, 2h \int_0^{L_t} \left(\frac{dw(x)}{dt} \right)^2 dx \qquad [3.2]$$

where ρ and L_t are the mass density and the total length of the specimen, respectively, t represents the time and $w(x)$ the displacement field. The quasi-static approach may provide an adequate approximation to the dynamic problem if the contribution of kinetic energy is small.

Wang et al. (Wang et al., 1995) have suggested that the dynamic fracture behaviour of materials depends on the balance between the energy released by the structure over a unit area of crack propagation (G) and the material resistance (R), which can be viewed as the energy dissipated in creating the fracture surface. When unstable crack growth occurs, the difference G-R is converted into kinetic energy. If G increases with crack growth the crack speed also increases because more energy is available. Crack arrest will occur when G becomes lower than R and, consequently, no kinetic energy is available for crack growth. Thus, it can be affirmed that fracture stability depends on the variations of the strain energy release rate and the materials resistance during crack growth. On the other hand, the fracture resistance of polymer composites is generally sensitive to loading rate. Under impact load or during rapid delamination growth, the strain rate at the crack tip can be very high and the material toughness significantly reduced. The fracture surface exhibited ductile tearing and large scale plastic deformation of the matrix. The dynamic fracture surface in the initiation exhibits less plastic deformation; during propagation even less deformation is observed. It was also verified that plastic zone size at the crack tip diminishes with increasing rate. Consequently, the decrease in mode II interlaminar fracture toughness is attributed to a transition from ductile to brittle matrix dominated failure with increasing rate.

The decreasing trend of toughness with increase of crack speed was also observed by Kumar et al. (Kumar et al., 1998). The authors used a combination of numerical and experimental techniques on the DCB specimens to carry out dynamic interlaminar toughness measurements of unidirectional glass fiber epoxy laminate. They observed a sharp decrease of dynamic toughness values relatively to the quasi-static ones. In fact, they measured dynamic toughness initiation values of 90-230 N/m^2 against quasi-static values of 344-478 N/m^2. Propagation values of 0-50 N/m^2 were obtained for crack speed ranging between 622-1016 m/s.

The majority of the experimental studies consider unidirectional laminates. Lambros et al. (Lambros et al., 1997) performed an experimental investigation of dynamic crack initiation and growth in unidirectional fiber-reinforced polymeric-matrix thick composite plates. Edge-notched plates were impacted in a one-point bend configuration using a drop-weight tower. Using an optical method the authors carried out a real-time visualization of dynamic fracture initiation and growth for crack speeds up to 900 m/s. They verified that the elastic constants of the used material are rate sensitive and the measured fracture toughness values are close to the typical ones of epoxies. This was considered consistent, because in unidirectional lay-ups crack initiation and growth occurs in the matrix.

Tsai et al., (Tsai et al., 2001) used a modified ENF specimen to determine the mode II dominated dynamic delamination fracture toughness of fiber composites at high crack propagation speeds. A strip of adhesive film with higher toughness was placed at the tip of interlaminar crack created during laminate lay-up. The objective was to delay the

onset of crack extension and produce crack propagation at high speeds (700 m/s). Sixteen pure aluminum conductive lines were put on the specimen edge side using the vapor deposition technique, to carry out crack speed measurements. The authors concluded that the mode II dynamic energy release rate of unidirectional S2/8553 glass/epoxy composite seems to be insensitive to crack speed within the range of 350 and 700 m/s. The authors also simulated mixed mode crack propagation by moving the pre-crack from the mid-plane to 1/3 of the ENF specimen thickness of unidirectional AS4/3501-6 carbon/epoxy laminates. The maximum induced crack speed produced was 1100 m/s. They found that that the critical dynamic energy release rate is not affected by the crack speed and lies within the scatter range of the respective static values.

For numerical simulations of the dynamic crack propagation the cohesive damage models emerge as the most promising tools. The major difficulty is the incorporation of the rate-dependent effects in the constitutive laws. Corigliano et al. (Corigliano et al., 2003) developed a cohesive crack model with a rate-dependent exponential interface law to simulate the nucleation and propagation of cracks subjected to mode I dynamic loading. The model is able to simulate the rate-dependent effects on the dynamic debonding process in composites. The authors concluded that the softening process occurs under larger relative displacements in comparison to rate-independent models. They verified that the type of rate-dependency can affect dynamic crack processes, namely the time to rupture and fracture energy. They also state that these effects diminish when inertial terms become dominant.

In summary, dynamic fracture toughness characterization of composite materials has been the centre of attention of several authors with no apparent consensus on the results.

Although the majority of the studies point to a decrease of the fracture toughness with increasing load rate there is no unanimity about this topic. Some authors observed the opposite trend (Corigliano et al., 2003) and others detected no remarkable influence of crack speed on toughness (Tsai et al., 2001). Although some of these discrepancies can eventually be explained by different behaviour of the tested materials, and the attained crack speed values, it is obvious that more profound studies about the subject are necessary.

4. Conclusions

Interlaminar fracture characterization of composites in mode II acquires special relevancy namely under transverse loading such as low velocity impact. Up to now there is no standardized test in order to measure the critical strain energy release rate in mode II. Due to their simplicity, the ENF and ELS tests become the principal candidates to standardization. However, they present a common difficulty associated with crack monitoring during propagation which is fundamental to obtaining the *R*-curves, following the classical data reduction schemes. To surmount these difficulties a new data reduction scheme based on specimen compliance is proposed. The method does not require crack length measurement during propagation, and accounts for the effects of the quite extensive FPZ on the measured critical strain energy release rate. Numerical simulations of the ENF and ELS tests demonstrated the adequacy and suitability of the proposed method to obtain the mode II *R*-curves of composites. Due to its simplicity the ENF test is proposed for standardization.

Little work has been done on dynamic fracture of composite materials, namely under mode II loading. This is due to experimental difficulties related to inducing high crack

speeds in a monitored way. Although the majority of the published works point to a decrease of the dynamic toughness with increase of crack speed, it appears that dynamic toughness can be similar to the respective quasi-static value up to a given crack speed (Tsai et al., 2001). Undoubtedly, more research about this topic is necessary. In fact, an unsafe structural design can occur if the quasi-static values of toughness are used in a dynamically loaded structure.

Acknowledgements

The author thanks Professors Alfredo B. de Morais (UA, Portugal), José Morais (UTAD, Portugal) and Manuel Silva for their valorous collaboration, advices and discussion about the matters included in this chapter. The author also thanks the Portuguese Foundation for Science and Technology for supporting part of the work here presented, through the research project POCI/EME/56567/2004.

References

Barrett JD, Foschi RO (1977), 'Mode II stress-intensity factors for cracked wood beams', *Engng. Fract. Mech*., 9: 371-378.

Carlsson LA, Gillespie JW, Pipes RB (1986), 'On the analysis and design of the end notched flexure (ENF) specimen for mode II testing', *J Compos Mater*, 20;594–604.

Choi H Y, Chang F K (1992), 'A model for predicting damage in graphite/epoxy laminated composites resulting from low-velocity point impact', *J Compos Mater*, 26; 2134-2169.

Corigliano A, Mariani S, Pandolfi A (2003), 'Numerical modelling of rate-dependent debonding processes in composites', *Compos. Struct*., 61;39-50.

Davidson BD, Sun X (2005), 'Effects of friction, geometry and fixture compliance on the perceived compliance from three- and four-point bend end-notched flexure tests', *J. Reinf. Plastics Compos.*, 24;1611-1628.

Davies P, Blackman BRK, Brunner AJ (2001), Mode II delamination. In: Moore DR, Pavan A, Williams JG, editors. *Fracture mechanics testing methods for polymers adhesives and composites*. Amsterdam, London, New York: Elsevier; 307-334.

de Morais AB, Pereira AB (2007), 'Application of the effective crack method to mode I and mode II interlaminar fracture of carbon/epoxy unidirectional laminates', *Composites Part A: Applied Science and Manufacturing* 38;785-794.

de Moura MFSF, Silva MAL, de Morais AB, Morais JJL (2006), 'Equivalent crack based mode II fracture characterization of wood', *Engng. Fract. Mech*. 73;978–993.

Guo C, Sun CT (1998), 'Dynamic mode-I crack propagation in a carbon/epoxy composite', *Composites Science and Technology* 58;1405-1410.

Kageyama K, Kikuchi M, Yanagisawa N (1991), 'Stabilized end notched flexure test: characterization of mode II interlaminar crack growth'. In: O'Brien TK, editor. *Composite Materials: Fatigue and Fracture*. ASTM STP 1110, Vol. 3. Philadelphia:. p. 210–25.

Kanninen MF, Popelar CH (1985), 'Advanced Fracture Mechanics', Oxford University Press.

Kumar P, Narayanan MD (1993), 'Energy dissipation of projectile impacted panels of glass fabric reinforced composites', *Compos. Struct*., 15;75–90.

Kumar P, Kishore NN (1998), 'Initiation and propagation toughness of delamination crack uncder an impact load', *J. Mech. Phys. Solids* 46;1773-1787.

Lambros J, Rosakis AJ (1997), 'Dynamic crack initiation and growth in thick unidirectional graphite/epoxy plates', *Composites Science & Technology*, 57;55-65.

Maikuma H, Gillespie JW, Wilkins DJ (1990), 'Mode II interlaminar fracture of the center notch flexural specimen under impact loading', *J. Compos. Mater.*, 24;124-149.

Schuecker C, Davidson BD (2000), 'Effect of friction on the perceived mode II delamination toughness from three and four point bend end notched flexure tests', ASTM STP,1383;334–344.

Silva MAL (2006), 'Estudo das Propriedades de Fractura em Modo II e em Modo III da Madeira de Pinus pinaster Ait.', Master Thesis, FEUP, Porto.

Silva MAL, Morais JJL, de Moura MFSF, Lousada JL (2007), 'Mode II wood fracture characterization using the ELS test', *Eng. Fract. Mech.*, 74:2133-2147.

Tanaka K, Kageyama K, Hojo M (1995), 'Prestandardization study on mode II interlaminar fracture toughness test for CFRP in Japan', *Composites*,26:243–255.

Tsai JL, Guo C, Sun CT (2001), 'Dynamic delamination fracture toughness in unidirectional polymeric composites', *Composites Science & Technology*, 61;87-94.

Yoshihara H, Ohta M (2000), 'Measurement of mode II fracture toughness of wood by the end-notched flexure test. *J Wood Sci*.;46:273–278.

Yoshihara H (2004), 'Mode II *R*-curve of wood measured by 4-ENF test', *Engng. Fract. Mech*., 71;2065–2077.

Wang H, Vu-Khanh T (1991), 'Impact-induced delamination in [05, 905, 05] carbon fiber/Polyetheretherketone composite laminates', Polymer Engineering and Science, 31;1301-1309.

Wang H, Vu-Khanh T (1995), 'Fracture mechanics and mechanisms of impact-induced delamination in laminated composites', *J. Compos. Mater.*, 29;156-178.

Wang H, Vu-Khanh T (1996), 'Use of end-loaded-split (ELS) test to study stable fracture behaviour of composites under mode II loading', *Compos. Struct*., 36;71–79.

Wang Y, Williams JG (1992), ‘Corrections for Mode II Fracture Toughness Specimens of Composite Materials’, *Composites Science & Technology*, 43;251-256.

Figures

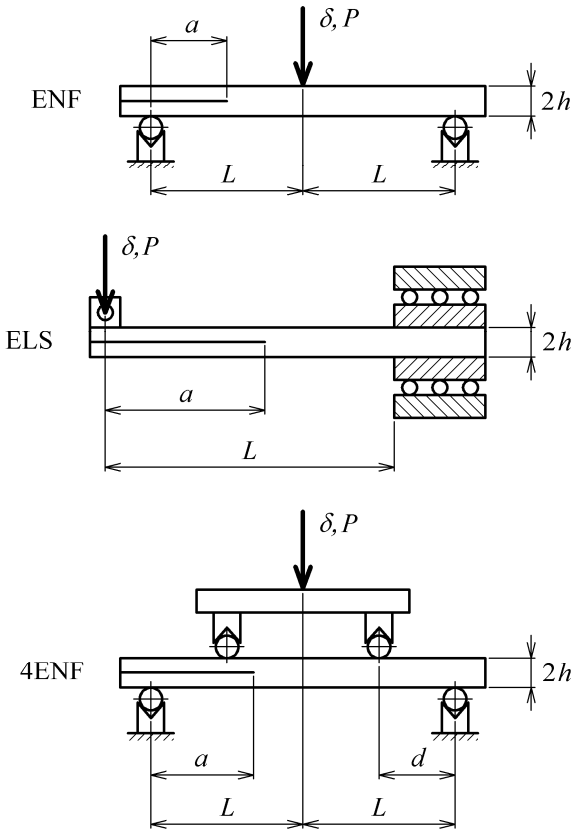

Figure 2.1 Schematic representations of the mode II tests.

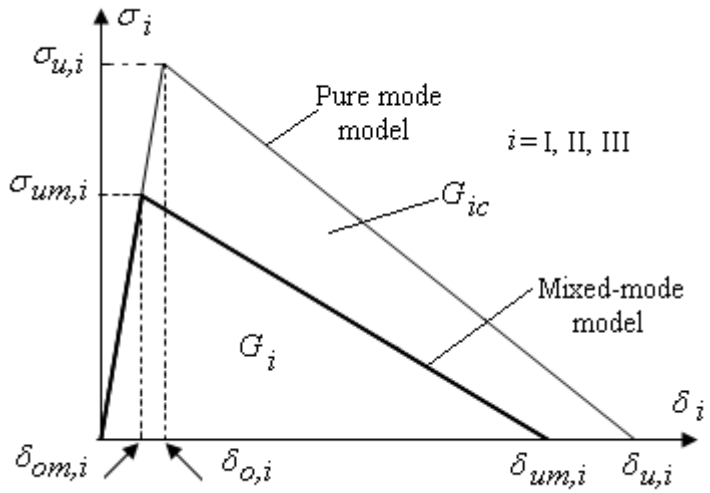

Figure 2.2 - Pure and mixed-mode damage model.

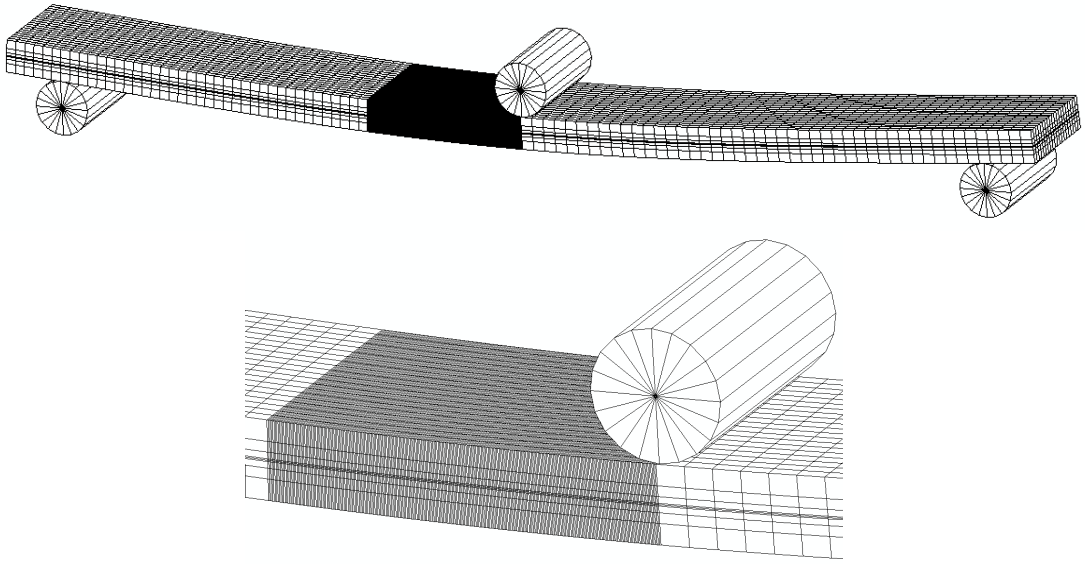

Figure 2.3 – The mesh used for the ENF test: global view and detail of the refined mesh at the region of crack initiation and growth.

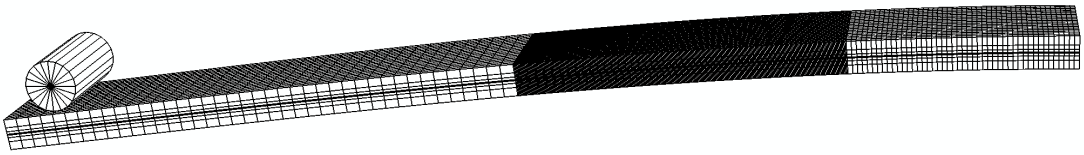

Figure 2.4 – The mesh used for the ELS test.

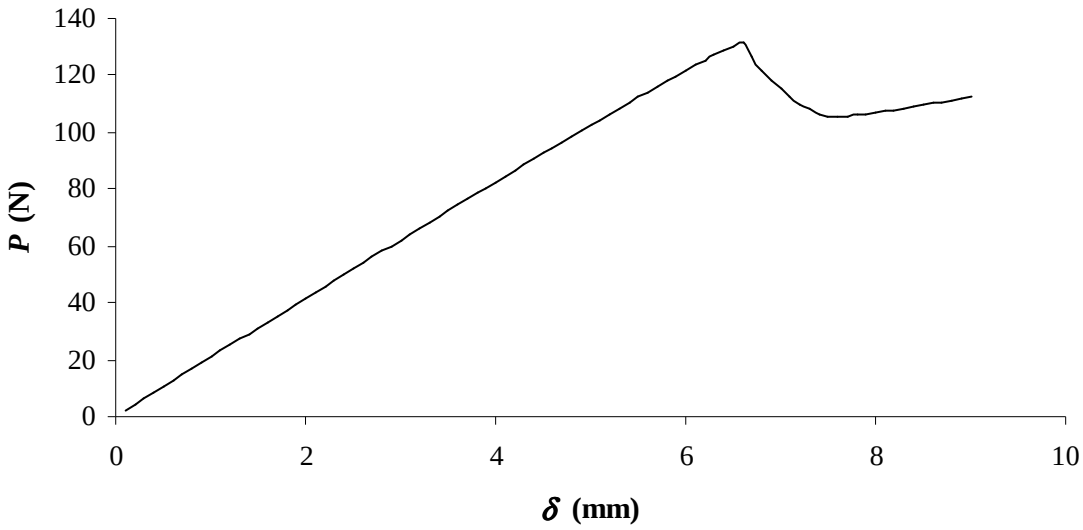

Figure 2.5 – P-δ curve of the ENF specimen.

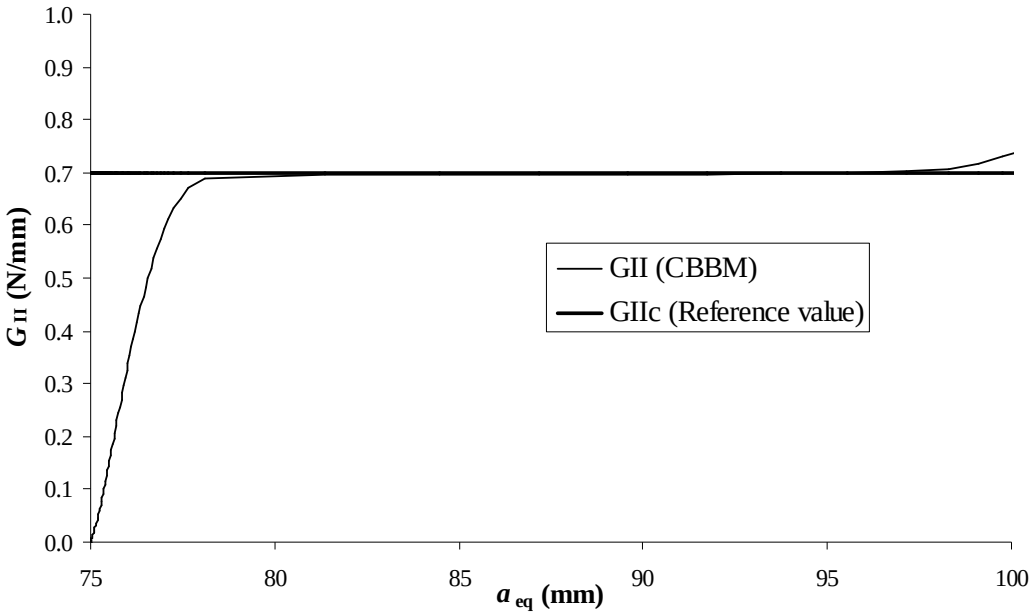

Figure 2.6 – *R*-curve of the ENF specimen.

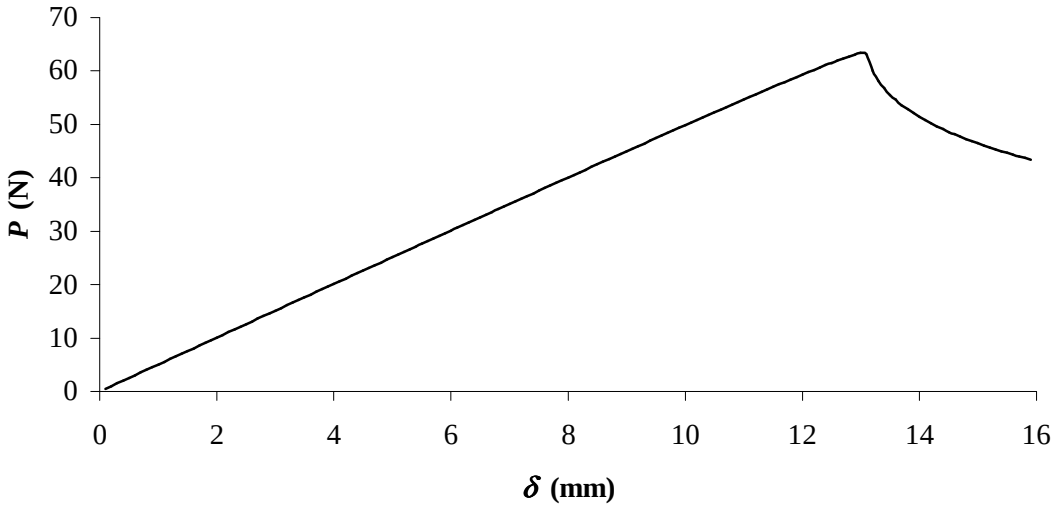

Figure 2.7 – *P*-δ curve of the ELS specimen.

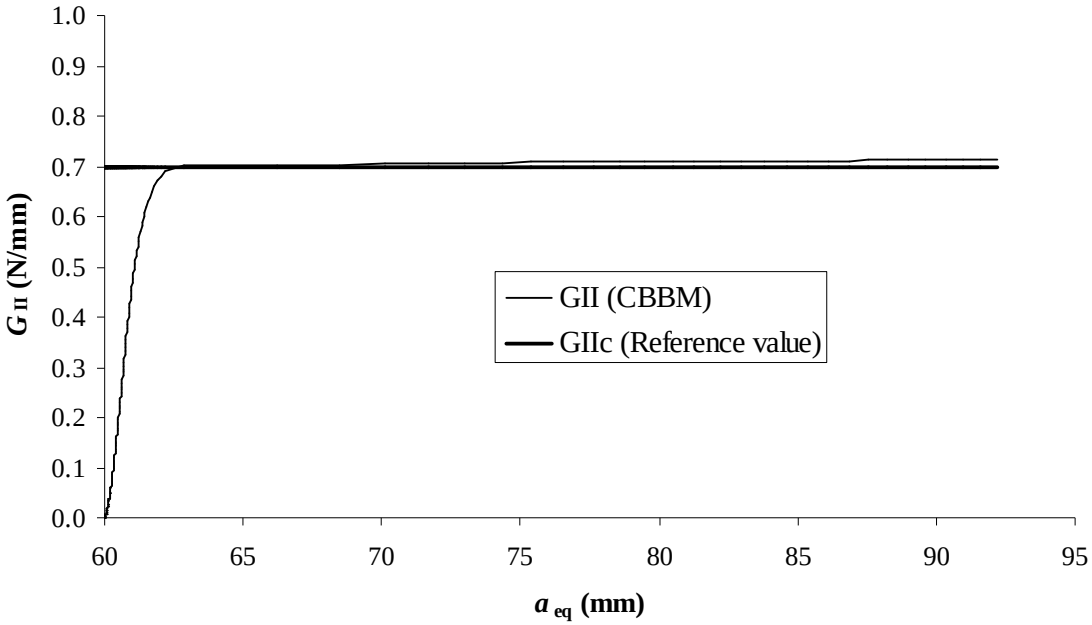

Figure 2.8 – *R*-curve of the ELS specimen.

Tables

Table 2.1. Specimens' geometry

	L (mm)	b (mm)	h (mm)	a_0 (mm)
ENF	100	10	1.5	75
ELS	100	10	1.5	60

Table 2.2. Elastic properties

E_1 (GPa)	$E_2 = E_3$ (GPa)	$\nu_{12}=\nu_{13}$	ν_{23}	$G_{12}= G_{13}$ (GPa)	G_{23} (GPa)
150	11	0.25	0.4	6	3.9

Table 2.3. Strength properties.

$\sigma_{u,i}$ (i=I,II,III) (MPa)	G_{Ic} (N/mm)	G_{IIc} (N/mm)	G_{IIIc} (N/mm)
40	0.3	0.7	1.0